

# A novel second subproblem for two arbitrary axes of robots

Haixia Wang<sup>1,2</sup>, Xiao Lu<sup>1,2</sup>, Ziyi Zhang<sup>3</sup>, Yuxia Li<sup>1,2</sup>,  
Chunyang Sheng<sup>2</sup> and Li Gao<sup>4</sup>

## Abstract

The Paden–kahan subproblem is a simple and flexible method to solve the closed-form inverse resolution but limited by the geometrical structure of robots, which is very difficult to be kept because of processing and installation. Therefore, a closed-form solution on arbitrary configurations is an important issue in the field of robotic inverse kinematics. A novel second subproblem is firstly proposed in this study based on the product-of-exponentials model adapting to the two arbitrary axes without geometric constraints (parallel, vertical, disjoint, and so on). Furthermore, the algebraic methods involving the basic properties of the screw theory and Rodrigues' rotation formula are employed for the solution, which makes the constraint equations of the second subproblem solvable for arbitrary configurations. This methodology can be applied to the inverse solutions of 5-degree-of-freedom robots that satisfies the Pieper criterion and can express the inverse solutions via two common formulas. Finally, the simulation and the real-world experiment demonstrated the accuracy of the method and the validity, respectively.

## Keywords

Inverse kinematics, closed-form resolution, POE model, screw theory, Rodrigues' rotation formula

Date received: 31 March 2017; accepted: 30 January 2018

Topic: Robot Manipulation and Control

Topic Editor: Andrey V Savkin

Associate Editor: Jayantha Katupitiya

## Introduction

The mapping relationship between the end effector and the joint angles of robots, referred to as a robot kinematics model, is very important in robot applications.<sup>1</sup> This relationship can be defined as forward or inverse kinematics, wherein the forward kinematics is to build the relationship in terms of the position and orientation of the end effector from the joint angles and can be easily determined by the link parameters and joint variables of a robot. Conversely, inverse kinematics (IK), which resolves the joint angles from the model based on the position and orientation of the end effector, is a nonlinear and configuration-dependent problem that may have multiple solutions.<sup>2</sup>

As solving the IK problem is significantly complicated, a closed-form inverse solution is desirable because it offers

<sup>1</sup> Key Laboratory for Robot and Intelligent Technology of Shandong Province, Shandong University of Science and Technology, Qingdao, China

<sup>2</sup> College of Electrical Engineering and Automation, Shandong University of Science and Technology, Qingdao, China

<sup>3</sup> College of Mathematics and Systems Science, Shandong University of Science and Technology, Qingdao, China

<sup>4</sup> College of Mechanical and Electronic Engineering, Shandong University of Science and Technology, Qingdao, China

## Corresponding author:

Haixia Wang, Key Laboratory for Robot and Intelligent Technology of Shandong Province, College of Electrical Engineering and Automation, Shandong University of Science and Technology, Qingdao 266590, China. Email: hxwang@sdust.edu.cn



fast computational speed and high precision.<sup>3</sup> However, robots must satisfy the Pieper criterion, which requires the paralleling of the three adjacent joint axes or the intersection of these joint axes at a single point.<sup>4</sup> Fortunately, most commercially available multi-joint robots satisfy this criterion. Additionally, there are several widely used methods to solve IK problems, such as Paul's inverse transformation,<sup>2</sup> Pieper's method,<sup>4</sup> and Paden–Kahan subproblems.<sup>5</sup> The first two methods are based on the Denavit–Hartenberg (D-H) model and require a large number of formula derivations and configuration-specific recalculations of solutions.<sup>6</sup> The Paden–Kahan method is based on the product-of-exponentials (POE) model, which decomposes a full manipulator into three classes of subproblems that can be easily solved, and every subproblem includes several types, and there are 28 types for three classes,<sup>7</sup> which consequently make the inverse solution to be easily obtained by assembling several subproblems according to the configuration. Evidently, the Paden–Kahan method is flexible, simple, geometrically meaningful, and numerically stable.<sup>3,7</sup> Moreover, because of these advantages, it can be widely applied in various research areas.<sup>8–11</sup>

Although it possesses the benefit of being more adaptable than other conventional methods, the types of existing subproblems are all based on the geometric relationships of adjacent axes such as intersecting,<sup>3,7,12</sup> parallel,<sup>13,14</sup> and different vertical surfaces.<sup>15</sup> However, in practice, the above relationships are hard to be kept during the process of machining and installing, and it limits the range of applicability of robots. In order to resolve this problem, a new second subproblem (new Sub-2) without geometric constraints is developed. New Sub-2 utilizes the new first subproblem (new Sub-1) to reduce the five IK solutions for 5-degree-of-freedom (5-DOF) robots into two formulas. It is important that this new method can be applied in other fields, such as semi-vehicle suspension systems<sup>16</sup> and 2-DOF quarter-car suspension systems.<sup>17</sup>

The remaining sections of this article are arranged as follows: first, background knowledge on the aforementioned problem is presented in the form of a mathematical description of the second subproblem, properties of the screw theory, and two important lemmas. The subsequent section details the derivation process of the novel first and second subproblems. Next, the closed-form inverse solutions of the 5-DOF robots are provided. The succeeding section demonstrates the practicability of the first and second subproblems developed in this study by presenting analysis and comparative results of simulation and actual experimentation. In the final section, the significance of the results and future work is discussed.

## Background knowledge

### Mathematical description of the second subproblem

As shown in Figure 1, the second subproblem is defined as a rotation of  $\mathbf{p}_1$  about  $\hat{\xi}_2(\omega_2, \mathbf{r}_2)$ , followed by a rotation

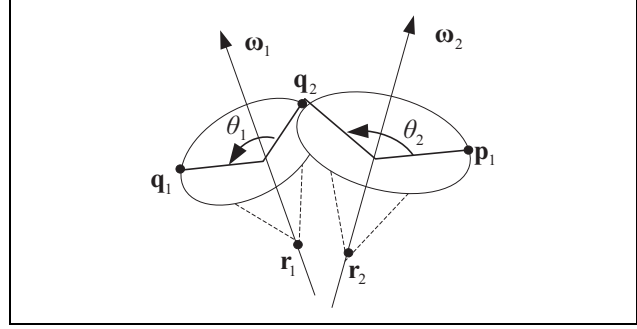


Figure 1. Second subproblem.

about the axis of  $\hat{\xi}_1(\omega_1, \mathbf{r}_1)$ , such that the final location of  $\mathbf{p}_1$  is coincident with  $\mathbf{q}_1$ . It can be described as

$$\tilde{\mathbf{q}}_1 = e^{\theta_1 \hat{\xi}_1} e^{\theta_2 \hat{\xi}_2} \tilde{\mathbf{p}}_1 \quad (1)$$

where  $\tilde{\mathbf{p}}_1$  and  $\tilde{\mathbf{q}}_1$  are the respective homogenous coordinates of space points  $\mathbf{p}_1$  and  $\mathbf{q}_1$ , and  $\hat{\xi}_i (i = 1, 2)$  are the joint twists of an instantaneous motion with the unit direction vector  $\omega_i \in \mathcal{R}^{3 \times 1}$  and the arbitrary point of the axis  $\mathbf{r}_i \in \mathcal{R}^{3 \times 1}$ ; additionally,  $e^{\theta \hat{\xi}}$  denotes rigid motion. For a revolute joint, the  $e^{\theta \hat{\xi}}$  is expressed as

$$e^{\theta \hat{\xi}} = \begin{bmatrix} e^{\theta \hat{\omega}} & (\mathbf{I} - e^{\theta \hat{\omega}}) \mathbf{r} \\ \mathbf{0} & 1 \end{bmatrix} \quad (2)$$

where  $\mathbf{I}$  is a  $3 \times 3$  unit matrix,  $e^{\theta \hat{\omega}}$  is a rotation matrix, which can be expressed via Rodrigues' formula, which is an efficient algorithm for rotating a vector in space, given an axis  $\omega$  and angle  $\theta$  of rotation, as shown in equation (3).

$$e^{\theta \hat{\omega}} = \mathbf{R} = \mathbf{I} + \sin \theta \hat{\omega} + (1 - \cos \theta) \hat{\omega}^2 \quad (3)$$

where  $\hat{\omega}$  is the skew-symmetric matrix of  $\omega = [\omega_x, \omega_y, \omega_z]^T$ , which is explicitly written as

$$\hat{\omega} = \begin{bmatrix} 0 & -\omega_z & \omega_y \\ \omega_z & 0 & -\omega_x \\ -\omega_y & \omega_x & 0 \end{bmatrix}$$

### Two related lemmas

In order to facilitate the understanding of the derivation process of the novel subproblems, two important lemmas are provided here for application in a later section.

**Lemma 1.** If a vector  $\mathbf{p}$  rotates an angle  $\theta$  by  $\hat{\xi}(\omega, \mathbf{r})$  toward  $\mathbf{q}$ , which can be expressed as  $\tilde{\mathbf{q}} = e^{\theta \hat{\xi}} \tilde{\mathbf{p}}$ , then the relationship between  $\mathbf{p}$  and  $\mathbf{q}$  can be described as

$$\mathbf{q} = e^{\theta \hat{\omega}} (\mathbf{p} - \mathbf{r}) + \mathbf{r} \quad (4)$$

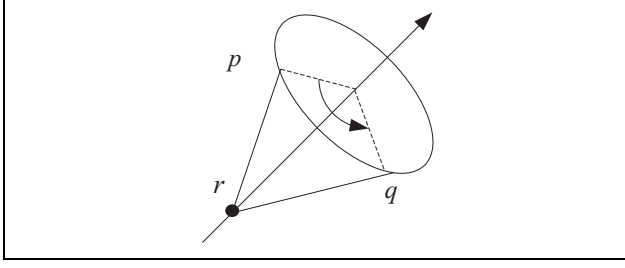


**Figure 2.** First subproblem.

**Lemma 2.** Applying equation  $x \sin \theta + y \cos \theta = z$  about the variable  $\theta$  yields the following result

$$\theta = A \tan 2(z, \pm \sqrt{x^2 + y^2 - z^2}) - A \tan 2(y, x) \quad (5)$$

Proofs of Lemmas 1 and 2 can be found in Appendix 1.

## Calculation of novel subproblems

The existing methods can be applied in the robots with some special geometric relationship; however, the resulting expressions vary according to the robot configuration. Because of this, a general and simple expression is more practical in robot applications. Therefore, a novel method combining the geometric and algebraic methods is introduced, in which the explicit geometric relationship, such as the equidistant relationship before and after the rotation, is utilized to obtain the constraint equations, while the algebraic method involving the basic properties of the screw theory and Rodrigues' rotation formula is used to resolve the equations.

### Solving the new Sub-1 using algebraic methods

As can be ascertained from Figure 2

$$\tilde{\mathbf{q}} = e^{\theta \hat{\mathbf{e}}} \tilde{\mathbf{p}} \quad (6)$$

Furthermore, according to Lemma 1

$$\mathbf{q} = e^{\theta \hat{\mathbf{\omega}}} (\mathbf{p} - \mathbf{r}) + \mathbf{r} \quad (7)$$

Then, substituting the Rodrigues' formula for  $e^{\theta \hat{\mathbf{\omega}}}$  into equation (7) yields the following:

$$\mathbf{x} \sin \theta + \mathbf{y} \cos \theta = \mathbf{z} \quad (8)$$

where

$$\begin{aligned} \mathbf{x} &= \hat{\mathbf{\omega}} (\mathbf{p} - \mathbf{r}) \in \mathfrak{R}^{3 \times 1} \\ \mathbf{y} &= -\hat{\mathbf{\omega}}^2 (\mathbf{p} - \mathbf{r}) \in \mathfrak{R}^{3 \times 1} \\ \mathbf{z} &= \mathbf{q} - \mathbf{p} - \hat{\mathbf{\omega}}^2 (\mathbf{p} - \mathbf{r}) \in \mathfrak{R}^{3 \times 1} \end{aligned}$$

Because  $\mathbf{x}^T \mathbf{y} = 0$  and  $\mathbf{x}^T \mathbf{x} = \mathbf{y}^T \mathbf{y}$ , multiplying by  $\mathbf{x}^T$  and  $\mathbf{y}^T$ , respectively, on either side of equation (8), it holds that

$$\sin \theta = \frac{\mathbf{x}^T \mathbf{z}}{\mathbf{x}^T \mathbf{x}} \quad (9)$$

and

$$\cos \theta = \frac{\mathbf{y}^T \mathbf{z}}{\mathbf{y}^T \mathbf{y}} \quad (10)$$

Thus,  $\theta$  can be expressed as

$$\theta = \arctan \left( \frac{\mathbf{x}^T \mathbf{z}}{\mathbf{y}^T \mathbf{z}} \right) \quad (11)$$

This equation is new Sub-1.

### Solving the new Sub-2 using algebraic methods

As illustrated in Figure 1, the distance between  $\mathbf{p}_1$  and  $\mathbf{q}_2$  is preserved via rigid motions<sup>3</sup> and gives

$$\|\mathbf{q}_2 - \mathbf{r}_2\| = \|\mathbf{p}_1 - \mathbf{r}_2\| \quad (12)$$

Additionally, applying Lemma 1 yields

$$\mathbf{q}_2 = e^{-\theta_1 \hat{\mathbf{\omega}}_1} (\mathbf{q}_1 - \mathbf{r}_1) + \mathbf{r}_1 \quad (13)$$

Then, substituting equation (13) into equation (12) yields the following

$$\|e^{-\theta_1 \hat{\mathbf{\omega}}_1} (\mathbf{q}_1 - \mathbf{r}_1) + \mathbf{r}_1 - \mathbf{r}_2\| = \|\mathbf{p}_1 - \mathbf{r}_2\| \quad (14)$$

Squaring both sides of the above equation simplifies the formula to yield

$$x_1 \sin \theta_1 + y_1 \cos \theta_1 = z_1 \quad (15)$$

where

$$\begin{aligned} x_1 &= -(\mathbf{r}_1 - \mathbf{r}_2)^T \hat{\mathbf{\omega}}_1 (\mathbf{q}_1 - \mathbf{r}_1) \\ y_1 &= -(\mathbf{r}_1 - \mathbf{r}_2)^T \hat{\mathbf{\omega}}_1^2 (\mathbf{q}_1 - \mathbf{r}_1) \\ z_1 &= \frac{1}{2} (\|\mathbf{p}_1\|^2 - \|\mathbf{q}_1\|^2 - 2\mathbf{p}_1^T \mathbf{r}_2) \\ &\quad + \mathbf{q}_1^T \mathbf{r}_2 - (\mathbf{r}_1 - \mathbf{r}_2)^T \hat{\mathbf{\omega}}_1^2 (\mathbf{q}_1 - \mathbf{r}_1) \end{aligned}$$

According to Lemma 2,  $\theta_1$  can be directly obtained, as shown in equation (16).

$$\theta_1 = \arctan \left( \frac{\pm z_1}{\sqrt{x_1^2 + y_1^2 - z_1^2}} \right) - \arctan \left( \frac{y_1}{x_1} \right) \quad (16)$$

Because  $\theta_1$  is constant, the value of  $\mathbf{q}_2$  is further obtained from equation (13); therefore,  $\theta_2$  can be solved using new Sub-1, which is given as equation (11).

As expected, the above equation is adaptable to any case with two adjacent axes; however, it is important to note that the two points  $\mathbf{r}_1$  and  $\mathbf{r}_2$  located on the joint axes should satisfy the requirement for which  $\mathbf{r}_1 \neq \mathbf{r}_2 \neq \mathbf{r}_0$  when the two axes intersect, where  $\mathbf{r}_0$  is the intersection.

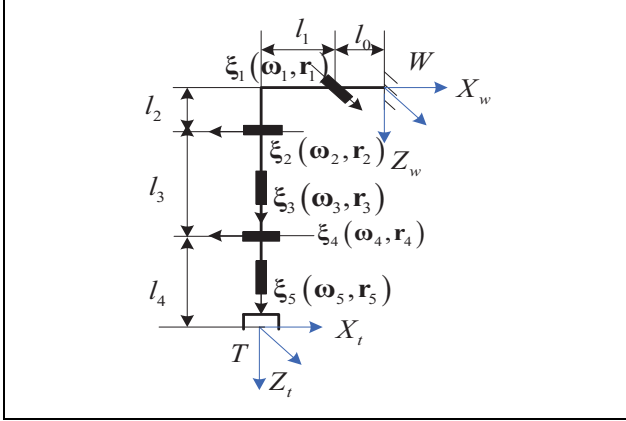


**Figure 3.** The structural diagram of a 5-DOF robot. 5-DOF: 5-degrees of freedom.

### Inverse solution of a 5-DOF robot

Figure 3 shows the structural diagram of a 5-DOF robot, including a shoulder joint, an elbow joint, and wrist joints, where the shoulder and elbow joints are two disjoint axes, and three joints of the wrist are intersecting; its POE model can be expressed as

$$\mathbf{g} = e^{\theta_1 \hat{\xi}_1} e^{\theta_2 \hat{\xi}_2} e^{\theta_3 \hat{\xi}_3} e^{\theta_4 \hat{\xi}_4} e^{\theta_5 \hat{\xi}_5} \quad (17)$$

where  $\mathbf{g} = \mathbf{g}_{wt}(\theta) \mathbf{g}_{wt}(\mathbf{0})^{-1} \mathbf{g}_{wt}(\mathbf{0})$ , and  $\mathbf{g}_{wt}(\theta)$  correspond to the initial and final posture (including position and orientation) of the end effector T frame under the world coordinate W. The twist parameters of the joints are as follows

$$\begin{aligned} \boldsymbol{\omega}_1 &= [0, 1, 0]^T, \boldsymbol{\omega}_2 = [-1, 0, 0]^T, \boldsymbol{\omega}_3 = [0, 0, 1], \\ \boldsymbol{\omega}_4 &= [-1, 0, 0]^T, \boldsymbol{\omega}_5 = [0, 0, 1], \mathbf{r}_1 = [l_0, 0, 0]^T, \\ \mathbf{r}_2 &= [-(l_0 + l_1), 0, l_2]^T, \mathbf{r}_3 = [-(l_0 + l_1), 0, l_2 + l_3]^T, \\ \mathbf{r}_4 &= \mathbf{r}_3 + \lambda_1 \boldsymbol{\omega}_4, \text{ and } \mathbf{r}_5 = \mathbf{r}_3 + \lambda_2 \boldsymbol{\omega}_5. \end{aligned}$$

The initial posture can be expressed as

$$\mathbf{g}_{wt}(\mathbf{0}) = \begin{bmatrix} \mathbf{I}_{3 \times 3} & \begin{bmatrix} -(l_0 + l_1) \\ 0 \\ l_2 + l_3 + l_4 \end{bmatrix} \\ \mathbf{0} & 1 \end{bmatrix}$$

Suppose  $\mathbf{g}_{wt}(\theta)$  is known, then we can calculate the five joint variables according to the new Sub-1 and the new Sub-2 by following the three steps below.

1. Eliminate the three intersecting wrist joints by using POE equation reduction techniques. Let  $\mathbf{r}_3$  be the point of interaction of wrist joints, then multiplying  $\tilde{\mathbf{r}}_3$  to the right side of equation (17) yields

$$\tilde{\mathbf{g}}\tilde{\mathbf{r}}_3 = e^{\theta_1 \hat{\xi}_1} e^{\theta_2 \hat{\xi}_2} e^{\theta_3 \hat{\xi}_3} e^{\theta_4 \hat{\xi}_4} e^{\theta_5 \hat{\xi}_5} \tilde{\mathbf{r}}_3 \quad (18)$$

As  $\tilde{\mathbf{r}} = e^{\theta \hat{\xi}} \tilde{\mathbf{r}}$ , if  $\tilde{\mathbf{r}}$  is on the axis of  $\hat{\xi}$ , the above equation can be rewritten as

$$\tilde{\mathbf{q}}_1 = e^{\theta_1 \hat{\xi}_1} e^{\theta_2 \hat{\xi}_2} \tilde{\mathbf{p}}_1 \quad (19)$$

where  $\tilde{\mathbf{q}}_1 = \mathbf{g} \tilde{\mathbf{p}}_1$  and  $\tilde{\mathbf{p}}_1 = \tilde{\mathbf{r}}_3$ , then  $\theta_1$  and  $\theta_2$  can be solved by using the new Sub-2.

2. Because  $\theta_1$  and  $\theta_2$  are known, equation (17) can be rewritten as

$$e^{-\theta_2 \hat{\xi}_2} e^{-\theta_1 \hat{\xi}_1} \mathbf{g} = e^{\theta_3 \hat{\xi}_3} e^{\theta_4 \hat{\xi}_4} e^{\theta_5 \hat{\xi}_5} \quad (20)$$

Setting  $\mathbf{r}_5$  on the axis of  $\hat{\xi}_5$ , and assuming  $\mathbf{r}_5 \neq \mathbf{r}_3$ , then right-multiplying  $\tilde{\mathbf{r}}_5$  yields

$$\tilde{\mathbf{q}}_3 = e^{\theta_3 \hat{\xi}_3} e^{\theta_4 \hat{\xi}_4} \tilde{\mathbf{p}}_3 \quad (21)$$

where  $\tilde{\mathbf{q}}_3 = e^{-\theta_2 \hat{\xi}_2} e^{-\theta_1 \hat{\xi}_1} \mathbf{g} \tilde{\mathbf{p}}_3$  and  $\tilde{\mathbf{p}}_3 = \tilde{\mathbf{r}}_5$ . In this manner,  $\theta_3$  and  $\theta_4$  can be obtained by applying the new Sub-2 equation.

3. Substituting  $\theta_1$ ,  $\theta_2$ ,  $\theta_3$ , and  $\theta_4$  into equation (17), gives

$$e^{-\theta_4 \hat{\xi}_4} e^{-\theta_3 \hat{\xi}_3} e^{-\theta_2 \hat{\xi}_2} e^{-\theta_1 \hat{\xi}_1} \mathbf{g} = e^{\theta_5 \hat{\xi}_5} \quad (22)$$

We can thus define a point  $\mathbf{p}_5$  out of  $\hat{\xi}_5$ ; then, right-multiplying  $\tilde{\mathbf{p}}_5$  into equation (22) yields

$$\tilde{\mathbf{q}}_5 = e^{\theta_5 \hat{\xi}_5} \tilde{\mathbf{p}}_5 \quad (23)$$

where  $\tilde{\mathbf{q}}_5 = e^{-\theta_4 \hat{\xi}_4} e^{-\theta_3 \hat{\xi}_3} e^{-\theta_2 \hat{\xi}_2} e^{-\theta_1 \hat{\xi}_1} \mathbf{g} \tilde{\mathbf{p}}_5$ .  $\theta_5$  can be solved via the new Sub-1 equation. Now that the expressions for all five inverse solutions have been derived, they can be expressed as

$$\theta_i = \arctan \left( \frac{\pm z_i}{\sqrt{x_i^2 + y_i^2 - z_i^2}} \right) - \arctan \left( \frac{y_i}{x_i} \right), \quad i = 1, 3 \quad (24)$$

$$\theta_j = \arctan \left( \frac{\mathbf{x}_j^T \mathbf{z}_j}{\mathbf{y}_j^T \mathbf{z}_j} \right), \quad j = 2, 4, 5 \quad (25)$$

where

$$\begin{aligned} x_i &= -(\mathbf{r}_i - \mathbf{r}_{i+1})^T \hat{\boldsymbol{\omega}}_i (\mathbf{q}_i - \mathbf{r}_i) \\ y_i &= -(\mathbf{r}_i - \mathbf{r}_{i+1})^T \hat{\boldsymbol{\omega}}_i^2 (\mathbf{q}_i - \mathbf{r}_i) \\ z_i &= \frac{1}{2} (\|\mathbf{p}_i\|^2 - \|\mathbf{q}_i\|^2 - 2\mathbf{p}_i^T \mathbf{r}_{i+1}) \\ &\quad + \mathbf{q}_i^T \mathbf{r}_{i+1} - (\mathbf{r}_i - \mathbf{r}_{i+1})^T \hat{\boldsymbol{\omega}}_i^2 (\mathbf{q}_i - \mathbf{r}_i) \\ \mathbf{x}_j &= \hat{\boldsymbol{\omega}}_j (\mathbf{p}_j - \mathbf{r}_j) \in \mathcal{R}^{3 \times 1} \\ \mathbf{y}_j &= -\hat{\boldsymbol{\omega}}_j^2 (\mathbf{p}_j - \mathbf{r}_j) \in \mathcal{R}^{3 \times 1} \\ \mathbf{z}_j &= \mathbf{q}_j - \mathbf{p}_j - \hat{\boldsymbol{\omega}}_j^2 (\mathbf{p}_j - \mathbf{r}_j) \in \mathcal{R}^{3 \times 1} \end{aligned}$$

**Table 1.** Four groups of solutions for a 5-DOF robot.

Joint No.	$\theta_1$	$\theta_2$	$\theta_3$	$\theta_4$	$\theta_5$
1	$-121.7921^\circ$	$-18.6339^\circ$	$51.0063^\circ$	$255.9895^\circ$	$40^\circ$
2	$-121.7921^\circ$	$-18.6339^\circ$	$125.9610^\circ$	$255.9895^\circ$	$40^\circ$
3	$5^\circ$	$-5^\circ$	$15^\circ$	$-5^\circ$	$40^\circ$
4	$5^\circ$	$-5^\circ$	$15^\circ$	$-5^\circ$	$40^\circ$

5-DOF: 5-degrees of freedom.

In these equations,  $\mathbf{q}_1, \mathbf{p}_1, \mathbf{q}_3, \mathbf{p}_3, \mathbf{q}_5$ , and  $\mathbf{p}_5$  are the same as above, and  $\tilde{\mathbf{q}}_2 = e^{-\theta_1 \hat{\xi}_1} \tilde{\mathbf{q}}_1$ ,  $\tilde{\mathbf{p}}_2 = \tilde{\mathbf{p}}_1$ ,  $\tilde{\mathbf{q}}_4 = e^{-\theta_3 \hat{\xi}_3} \tilde{\mathbf{q}}_3$ , and  $\tilde{\mathbf{p}}_4 = \tilde{\mathbf{p}}_3$ . It is important to note that the relationship  $x_i^2 + y_i^2 > z_i^2$  must be guaranteed by choosing the proper  $\mathbf{r}_i$  and  $\mathbf{r}_{i+1}$ ; furthermore, the quadrants of  $\theta_j$  can be determined according to the signs of  $\mathbf{x}_j^T \mathbf{z}_j$  and  $\mathbf{y}_j^T \mathbf{z}_j$ .

## Actual and simulated experiments

In order to verify the correctness and validity of the proposed method, we apply the new Sub-1 and new Sub-2 in actual and simulated experiments.

### Simulated experiment

The screw parameters of the 5-DOF robot illustrated in Figure 3 can be set as

$\boldsymbol{\omega}_1 = [0, 1, 0]^T$ ,  $\mathbf{r}_1 = [l_0, 0, 0]^T$ ,  $\boldsymbol{\omega}_2 = [-1, 0, 0]$ ,  $\mathbf{r}_2 = [-(l_0 + l_1), 0, l_2]^T$ ,  $\boldsymbol{\omega}_3 = [0, 0, 1]^T$ ,  $\mathbf{r}_3 = [-(l_0 + l_1), 0, l_2 + l_3]^T$ ,  $\boldsymbol{\omega}_4 = [-1, 0, 0]^T$ ,  $\mathbf{r}_4 = \mathbf{r}_3 + \lambda_1 \boldsymbol{\omega}_4$ ,  $\boldsymbol{\omega}_5 = [0, 0, 1]^T$ ,  $\mathbf{r}_5 = \mathbf{r}_3 + \lambda_2 \boldsymbol{\omega}_5$ ,  $\lambda_1 = 500$ , and  $\lambda_2 = 20$ . Next, by choosing a group of joint angles  $\theta = [5^\circ, -5^\circ, 15^\circ, -35^\circ, 40^\circ]$  and substituting these parameters into equation (17), we can obtain the posture of the end effector as shown below.

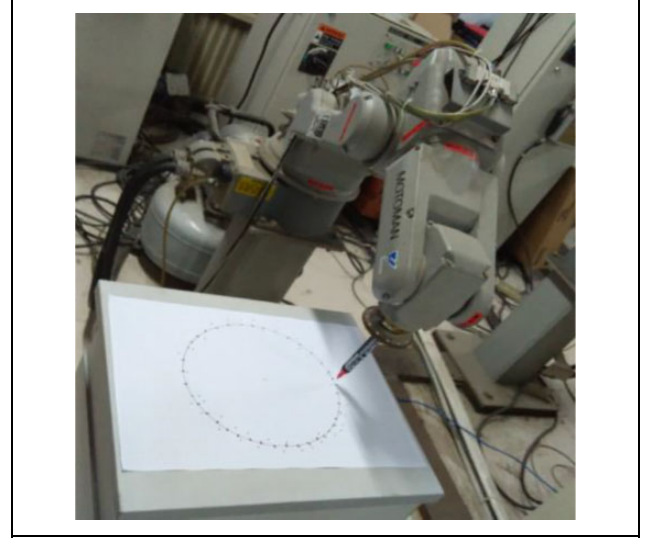
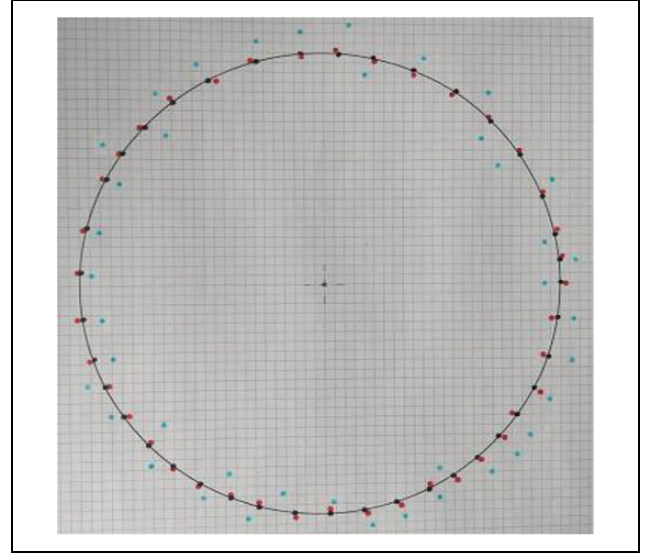
$$\mathbf{g} = \begin{bmatrix} 0.6387 & -0.7388 & 0.2148 & -82.3900 \\ 0.6720 & 0.3998 & -0.6233 & 219.1170 \\ 0.3746 & 0.5425 & 0.7519 & 130.8968 \\ 0 & 0 & 0 & 1 \end{bmatrix} \quad (26)$$

Subsequently, we can obtain all joint angles for the above posture by solving equations (24) and (25). There are four groups of solutions on the 5-DOF robot, as shown in Table 1.

Because the third and fourth group of angles listed in Table 1 are equivalent to the ground truth, the simulated experiment verifies the correctness of the proposed method.

### Actual experiment

For the practical test, we choose the 6-DOF Motoman-SV3X robot, YASKAWA company, as the testing platform, fix the wrist joints, and only allow movement of the waist, shoulder, and elbow joint, as shown in Figure 4; the end posture can be determined according to equation (27).

**Figure 4.** Experiment using the Motoman-SV3X.**Figure 5.** Tracking results.

$$\mathbf{g} = e^{\theta_1 \hat{\xi}_1} e^{\theta_2 \hat{\xi}_2} e^{\theta_3 \hat{\xi}_3} \quad (27)$$

Then, the three joint angles can be easily calculated via equations (24) and (25), where  $i = 1, j = 2, 3$ , and  $\tilde{\mathbf{q}}_1 = \mathbf{g} \tilde{\mathbf{p}}_1$ ,  $\tilde{\mathbf{p}}_1 = \tilde{\mathbf{r}}_3$ ,  $\tilde{\mathbf{q}}_2 = e^{-\theta_1 \hat{\xi}_1} \tilde{\mathbf{q}}_1$ ,  $\tilde{\mathbf{p}}_2 = \tilde{\mathbf{p}}_1$ ,  $\tilde{\mathbf{q}}_3 = e^{-\theta_2 \hat{\xi}_2} e^{-\theta_1 \hat{\xi}_1} \mathbf{g} \tilde{\mathbf{p}}_3$ , and  $\tilde{\mathbf{p}}_3$  is any point out of the axes  $\hat{\xi}_3$ . All screw parameters and  $\mathbf{g}_{wt}(\mathbf{0})$  can be calibrated by implementing the screw axis identification method.<sup>18</sup>

To confirm the effectiveness of the proposed method, we sample 40 points along the circle and then track these points by respectively utilizing the proposed method and a radial basis function neural network (RBFNN). The result is shown in Figure 5, where the black points represent the sampling points, the red points, and the blue points



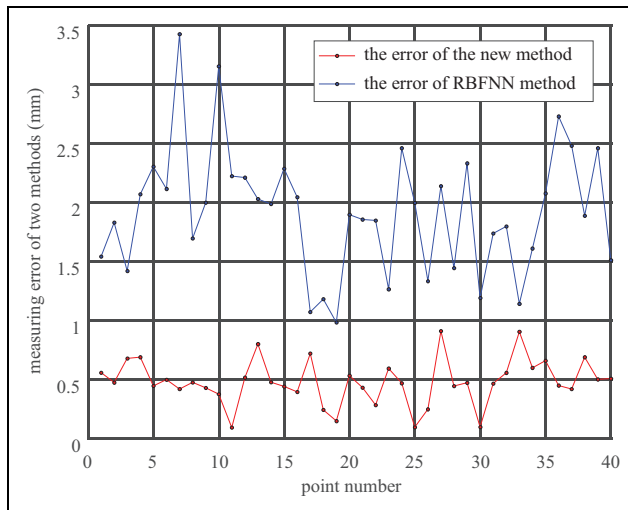


**Figure 6.** Comparative results of the two methods.

represent the tracking points obtained via our method and the RBFNN approach, respectively. The one defining the mean distance errors between the red and black points is  $e_1$  and the one between the blue and black points is  $e_2$ , as shown in Figure 6, the mean of  $e_1$  and  $e_2$  are 0.4794 mm and 1.9181 mm, respectively. Moreover, the respective computational speeds of the two methods are 2.31 and 12.681  $\mu$ s. Comparing the results obtained via our proposed method with those obtained via the RBFNN approach, an approximate fivefold increase in accuracy and five times increase in the computational speed relative to our method is observed.

## Conclusions

In this article, a novel second subproblem, which is suited to the problems with two arbitrary axes, has been proposed. On this basis, a general and simple closed-form solution for 5-DOF robots is also provided. In general, the proposed method utilizes a few features of the screw theory and Rodrigues' rotation formula to reduce the complexity of IK problems. Applying this methodology, three main advantages were determined, with the first advantage being that it can broaden the range of applicability of Paden-Kahan subproblems and can be applied to arbitrary 5-DOF robots satisfying the Pieper criterion, which has been demonstrated by adapting the methodology of an arbitrary 5-DOF robot. The second advantage is that it can simplify the problem-solving process for inverse kinematics, yielding only two formulas that can express the inverse solutions, thereby making the application of robot more convenient. Lastly, the methodology is stable and real-time owing to the adopted algebraic geometry algorithm, which takes into account the geometric relationships to build the constraint equation, and then solves the equation by employing algebraic approaches. Furthermore, the correctness and the validity of our method has been verified

via actual and simulated experiments, with the results showing that our method offers considerably higher accuracy and reduced computational speed as compared to the RBFNN method. However, although the proposed method yields clear advantages, a standard explaining how to satisfy the Pieper criterion or how to extend our method to be applicable to 6-DOF robots has not yet been determined. Therefore, a general solution for 6-DOF robots will be researched in future work.

## Acknowledgement

We are grateful to the reviewers for their valuable comments and suggestions which lead to improved presentation of this article.

## Declaration of conflicting interests

The author(s) declared no potential conflicts of interest with respect to the research, authorship, and/or publication of this article.

## Funding

The author(s) disclosed receipt of the following financial support for the research, authorship, and/or publication of this article: This work was supported by the National Natural Science Foundation of China (61503224, 61273197, 61773245, 61473177, 61603068), China Postdoctoral Science Foundation (2015M582115 and 2016T90640), SDUST Public visiting scholar, and Taishan Scholarship Construction Engineering.

## References

1. Spong M, Hutchinson S, and Vidyasagar M. *Robot modeling and control*. New York: Wiley, 2006. DOI: 10.1108/ir.2006.33.5.403.1.
2. Paul RP. *Robot manipulators: mathematics programming, and control*. Cambridge: MIT Press, 1981.
3. Murray RM, Li Z, Sastry SS, et al. *A mathematical introduction to robotic manipulation*. Boca Raton: CRC press, 1994.
4. Pieper DL. *The kinematics of manipulators under computer control*. Stanford Univ Ca Dept of Computer Science, PhD Thesis, Stanford University, CA, USA, 1968.
5. Paden BE. *Kinematics and Control Robot Manipulators*. PhD Thesis, University of California, Berkeley, USA, 1986.
6. Fu KS, Gonzalez RC, and Lee CS. *Robotics: control, sensing, vision and intelligence*. Singapore: McGrawHill Inc., 1987. DOI: 10.1177/002072098702400422.
7. Jie Z, Weizhong W, Yongsheng GA, et al. Generation of closed-form inverse kinematics for reconfigurable robots. *Fron Mech Eng* 2008; 3(1): 91–96. DOI: 10.1007/s11465-008-0013-6.
8. Pan Y, Wang H, Li X, et al. Adaptive command-filtered back stepping control of robot arms with compliant actuators. *IEEE Trans Control Syst Technol* 2017; (99): 1–8. DOI: 10.1109/tcst.2017.2695600.
9. Wang G, Sun T, Pan Y, et al. Adaptive neural network control for constrained robot manipulators. In: *International symposium on neural networks*, Springer, Cham, 2017, pp. 118–127. DOI: 10.1007/978-3-319-59081-3\_15.
10. Limón RC, Ibarra ZJM, and Armada RMA. Inverse kinematics of a humanoid robot with non-spherical hip: a hybrid

- algorithm approach. *Int J Adv Robot Syst* 2013; 10: 1–13. DOI: 10.5772/55464.
11. Mayyas M and Mellish R. A method for the automatic generation of inverse kinematic maps in modular robotic systems. *Int J Adv Robot Syst* 2016; 13(5): 1–15. DOI: 10.1177/1729881416662790.
  12. Yan G. *Decomposable closed form inverse kinematics for reconfigurable robots using product-of-exponentials formula*. Master's Thesis, Nanyang Technological University, Singapore, 2000.
  13. Chen IM and Gao Y. Closed-form inverse kinematics solver for reconfigurable robots. In: *IEEE international conference on robotics and automation*, Vol. 3, Seoul, South Korea, 21 May–26 May 2001, pp. 2395–2400. DOI:10.1109/robot.2001.932980.
  14. Chen Q, Zhu S, and Zhang X. Improved inverse kinematics algorithm using screw theory for a six-DOF robot manipulator. *Int J Adv Robot Syst* 2015; 12(10). DOI: 10.5772/60834.
  15. Yue-sheng T and Ai-Ping X. Extension of the second Paden-Kahan sub-problem and its application in the inverse kinematics of a manipulator. In: *IEEE conference on robotics, automation and mechatronics*, Chengdu, China, 21 September–24 September 2008, pp. 379–381. DOI:10.1109/ramech.2008.4681401.
  16. Zhang H, Zheng X, Yan H, et al. Co-design of event-triggered and distributed  $H_\infty$  filtering for active semi-vehicle suspension systems. *IEEE/ASME Trans Mech* 2017; 22(2): 1047–1058. DOI: 10.1109/tmech.2016.2646722.
  17. Zhang H, Hong Q, Yan H, et al. Event-based distributed  $H_\infty$  filtering networks of 2-DOF Quarter-car suspension systems. *IEEE Trans Industr Inform* 2017; 13(1): 312–321. DOI: 10.1109/tii.2016.2569566.
  18. Wang H, Shen S, and Lu X. A screw axis identification method for serial robot calibration based on the POE model. *Industr Robot Int J* 2012; 39(2): 146–153. DOI: 10.1108/01439911211201609.

## Appendix I

**Lemma 1.** If a vector  $\mathbf{p}$  rotates an angle  $\theta$  by  $\hat{\xi}(\omega, \mathbf{r})$  toward  $\mathbf{q}$ , which can be expressed as  $\tilde{\mathbf{q}} = e^{\theta \hat{\xi}} \tilde{\mathbf{p}}$ , then the relationship between  $\mathbf{p}$  and  $\mathbf{q}$  can be described as

$$\mathbf{q} = e^{\theta \hat{\omega}}(\mathbf{p} - \mathbf{r}) + \mathbf{r}$$

**Proof of Lemma 1.** According to the basic property of screw theory

$$\tilde{\mathbf{r}} = e^{\theta \hat{\xi}} \tilde{\mathbf{r}} \quad (\text{A.1})$$

Combining expression  $\tilde{\mathbf{q}} = e^{\theta \hat{\xi}} \tilde{\mathbf{p}}$ , it is a simple calculation to obtain

$$\tilde{\mathbf{q}} - \tilde{\mathbf{r}} = e^{\theta \hat{\xi}}(\tilde{\mathbf{p}} - \tilde{\mathbf{r}}) \quad (\text{A.2})$$

In terms of equation (A.2),  $e^{\theta \hat{\xi}}$  can be expressed as

$$e^{\theta \hat{\xi}} = \begin{bmatrix} e^{\theta \hat{\omega}} & \mathbf{t} \\ \mathbf{0} & 1 \end{bmatrix} \quad (\text{A.3})$$

where  $\mathbf{t} = (\mathbf{I}_{3 \times 3} - e^{\theta \hat{\omega}}) \mathbf{r}$ . Subsequently substituting equation (A.3) into equation (A.2) yields

$$\mathbf{q} = e^{\theta \hat{\omega}}(\mathbf{p} - \mathbf{r}) + \mathbf{r} \quad (\text{A.4})$$

Thus, Lemma 1 is proved.

**Lemma 2.** Applying equation  $x \sin \theta + y \cos \theta = z$  about the variable  $\theta$  yields the following result

$$\theta = A \tan 2(z, \pm \sqrt{x^2 + y^2 - z^2}) - A \tan 2(y, x)$$

**Proof of Lemma 2.** By setting  $x = \rho \cos \phi$  and  $y = \rho \sin \phi$ , the equation  $x \sin \theta + y \cos \theta = z$  can be rewritten as

$$\sin(\theta + \phi) = \frac{z}{\rho} \quad (\text{A.5})$$

where

$$\begin{aligned} \rho &= \sqrt{x^2 + y^2} \\ \phi &= A \tan 2(y, x) \end{aligned}$$

Similarly, there is

$$\cos(\theta + \phi) = \pm \sqrt{1 - \left(\frac{z}{\rho}\right)^2} \quad (\text{A.6})$$

and

$$\tan(\theta + \phi) = \pm \frac{z}{\sqrt{x^2 + y^2 - z^2}} \quad (\text{A.7})$$

From the above equations,  $\theta$  can be expressed as

$$\theta = A \tan 2(z, \pm \sqrt{x^2 + y^2 - z^2}) - A \tan 2(y, x) \quad (\text{A.8})$$

Thus, Lemma 2 is proved.